Journal of Materials Synthesis and Processing, Vol. 7, No. 4, 1999

Progress of the $NbAl_3$ Combustion Synthesis Reaction

Ricardo Mendes Leal Neto[1,2] and Paulo Iris Ferreira[1]

Parallelopipedal (60 × 10 × 10-mm) bars obtained by uniaxial compaction of Nb–Al powder mixtures with a stoichiometric $NbAl_3$ composition (75 a/o Al) were submitted to reaction synthesis using the SHS mode (self-propagating high-temperature synthesis). The experimental procedures used were such as to allow for the reaction ignition, propagation, and extinction at a certain plane along the bar length. The microstructure of the reacted bars was characterized by optical microscopy, scanning electron microscopy, and EDS. The various phases present along the bar length evidenced that the local composition was changed due to the presence of a molten aluminum flux during the reaction. All the observed phases are predicted by the Nb–Al equilibrium phase diagram. A possible explanation for the reaction sequence is advanced based on the experimental observations.

KEY WORDS: Combustion; SHS; intermetallics; aluminides.

1. INTRODUCTION

Since more than one century ago a great variety of materials has been synthesized using highly exothermic combustion reactions between elemental powder constituents [1]. During the last decade, the synthesis and processing of materials by this technique have been extended to a great variety of materials, and consequently, the number of practical and theoretical investigations in this area has increased significantly throughout the world. The number of published reviews [1–8] attests the strong interest on this subject. The technique is also referred to as self-propagating high-temperature synthesis (SHS), reaction sintering, and as-reaction synthesis. The method consists of inducing an exothermic chemical reaction in a mixture of reactants (solid, liquid, or gaseous), by increasing the temperature of the mixture to the point where the reaction is ignited and the heat generated by the reaction is enough to sustain it until all the reactants have been consumed. In general, this can be accomplished by two routes. In the first, referred to by the Soviet school [1] as SHS, the reaction is initiated in a localized region of the sample and is able to self-propagate as a combustion wave, converting the mixture of reactants to the products as it advances through the material. In the second, commonly referred to as the "thermal explosion mode" [2] or "simultaneous combustion" [8], the mixture is entirely heated up to the ignition temperature, at which the reaction starts simultaneously all over the mixture. Simultaneous combustion is especially necessary in those cases where the reactions have a low exothermy, making it difficult or even impossible for self-propagation to take place [2]. Generally, this is what usually occurs with reactions between metals, as those involved in the synthesis of intermetallic compounds [3], such as niobium trialuminide, $NbAl_3$, the subject of this work.

Many aspects concerning the synthesis and densification of niobium trialuminide have been investigated by the present authors [9–12]. As reported previously [11], a simple, qualitative model has been proposed for the synthesis reaction, based on the observations of the effects of the initial powder mixture composition on the reaction products. The intent of the present work is to pro-

[1] Materials Science and Engineering Department, Nuclear and Energetic Research Institute (IPEN), São Paulo, SP, Brazil.

[2] To whom correspondence should be addressed at P.O. Box 11049, São Paulo, SP 05422-970, Brazil. e-mail: lealneto@net.ipen.br.

1064-7562/99/0700-0245$16.00/0

vide a contribution to the understanding of the reaction evolution by performing experiments in which the reaction is interrupted by quickly cooling the specimen. For this purpose, a series of experiments leading to semireacted samples was envisaged. Microstructural analysis and phase identification performed on semireacted samples provided very elucidative details about the reaction step sequence.

2. EXPERIMENTAL

Experiments were conducted on parallelopipedal bars 10 × 10 mm in cross section and 60 mm long. Commercial gas atomized aluminum (99.7% purity grade) and hydride–dehydride niobium (99.5% purity grade) powders [11] were initially size classified by sieving (−325 mesh fraction was taken). The bars were obtained by uniaxially pressing at 100 MPa a mixture of Nb and Al powders weighted at the stoichiometric ratio for $NbAl_3$ (53.44 w/o of Nb and 46.56 w/o of Al) synthesis. A special device was built for igniting the bar at one of its ends. It consists of a quartz tube containing externally a Kanthal A1 wire resistor distributed along 40 mm of the central part of the tube. Ceramic rings were utilized for insulating the resistor wire. The assembly was covered with a coarse alumina blanket for preventing heating losses. The wire leads were connected to a variable a.c. power supply and fed by an electric current. Internal temperatures could be monitored by a type S thermocouple. Specimen temperature was measured by two thermocouples positioned inside a small cavity, ≈2 mm deep, drilled in two points of the bar. A thin alumina-based coating was used on the thermocouple beads to avoid their damage during the synthesis reaction. The small furnace built allowed well-controlled internal temperatures up to 1000°C. This upper limit temperature was enough to attain the objective, since the ignition temperature for the Nb–Al mixture is ~850°C, as reported previously [9]. To avoid gross specimen oxidation during heating and reaction, a flux of high-purity argon was utilized during the whole experiment. The ignition device was originally conceived to operate in both the horizontal and the vertical positions, to enable the water quenching of the bar. Preliminary experiments, however, showed that this procedure was not necessary, since the reaction extinguished after some propagation, even before reaching the cold end of the bar. Thus, in the majority of the experiments the bars were horizontally reacted.

The ignition of the sample involved the prior heating of the furnace to slightly above 850°C, followed by the introduction of one-third of the length of the bar into the hot zone. After the ignition and extinction of the reaction, the whole system was turned to the vertical position so that the reacted bar was quickly dropped in water. This procedure, besides rapidly cooling the specimen, also prevented gross oxidation of its nonreacted niobium–aluminum part. After visual inspection and photographic report, the bar was cut off longitudinally to obtain specimens for metallographic observations. Microstructural characterization consisted of optical and scanning electron microscopy (SEM). Energy-dispersive X-ray spectrometry (EDS) was also used for the chemical analysis of the phases present in the microstructure.

3. RESULTS AND DISCUSSION

3.1. Reaction Observation

In general, during specimen heating molten aluminum droplets were observed to be formed at the bar surface inside the furnace hot zone. These droplets, initially separated, joined and even formed a small pool at the contact region with the quartz tube as the temperature of the sample increased above the melting point of aluminum (660°C). Instants before the ignition, at a temperature well above the melting point of aluminum (850°C), these aluminum droplets were completely reabsorbed by the specimen. This occurrence was afterward taken as indicative of the imminence of the reaction. Similar observations were reported by Murray and German [13] and Kachelmyer *et al.* [14]. Murray and German [13], using fragments of compacted samples heated with a propane torch at a rate of several hundred kelvins per minute in air on an alumina boat, argued that droplet formation resulted from the lack of wetting of molten aluminum on niobium due to oxide formation on the surface of molten aluminum. According to these authors, wetting would be particularly inhibited on the external surface of the compact, and this situation would be reverted with the beginning of the reaction, which consumes aluminum. Kachelmyer *et al.* [14], in more elaborate combustion synthesis experiments performed under vacuum, reported a time interval between aluminum fusion and reaction ignition in which droplets were visualized. Based on their observations of a molten Al particle interaction with a Nb foil, these authors proposed that niobium wettability by aluminum is a function of temperature, so the reaction occurs well above the melting point of aluminum. In the present work, the time interval verified between aluminum melting (660°C) and reaction ignition (850°C), with the concurrent reabsorption of

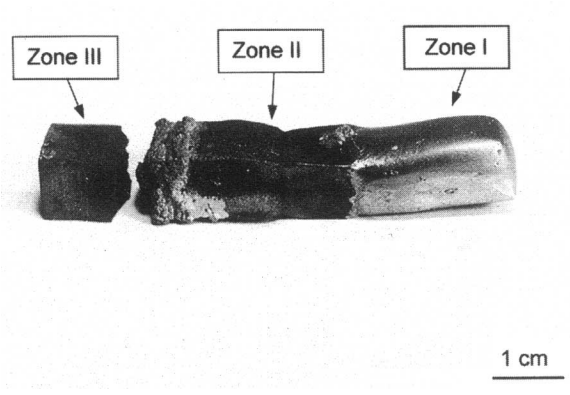

Fig. 1. Optical macrograph of the semireacted bar, showing zones I, II, and III as described in the text.

molten aluminum droplets by the sample, seems to favor the explanation proposed by Kachelmyer *et al.* [14].

3.2. Reacted Bar Microstructural Details

A general view of a semireacted bar is shown in Fig. 1. It is interesting to note that the geometry of the reacted bar suffered some changes. According to these changes, three distinct macroscopic zones are clearly defined, and in what follows, they are called zones I, II, and III, for better description of the various microstructural details observed. The first zone (zone I), presenting a shiny external surface, corresponds to the bar portion introduced into the hot zone of the furnace in which ignition first occurred and rapid combustion reaction propagation took place. Zone II, characterized by a dull external surface, corresponds to the bar part that was maintained out of the hot zone of the furnace. In this zone, the combustion wave propagated and extinguished after some extension. A noticeable central contraction of the bar is observed in this zone. The third zone (zone III) consists of the nonreacted part of the bar and has the normal as-compacted appearance.

The internal macrostructure observed along the central longitudinal section of the reacted bar is shown in Fig. 2. To describe better the results of microstructural observations along the bar volume, a reference coordinate system with the origin placed at point O (Fig. 2) is utilized. First, a uniform porosity is observed along the region between the origin (x = 0 mm) and the necked area (x = 30 mm). In general, the pores are spherical in shape, indicating the occurrence of internal pressurization. There is a wide distribution of pores. The largest

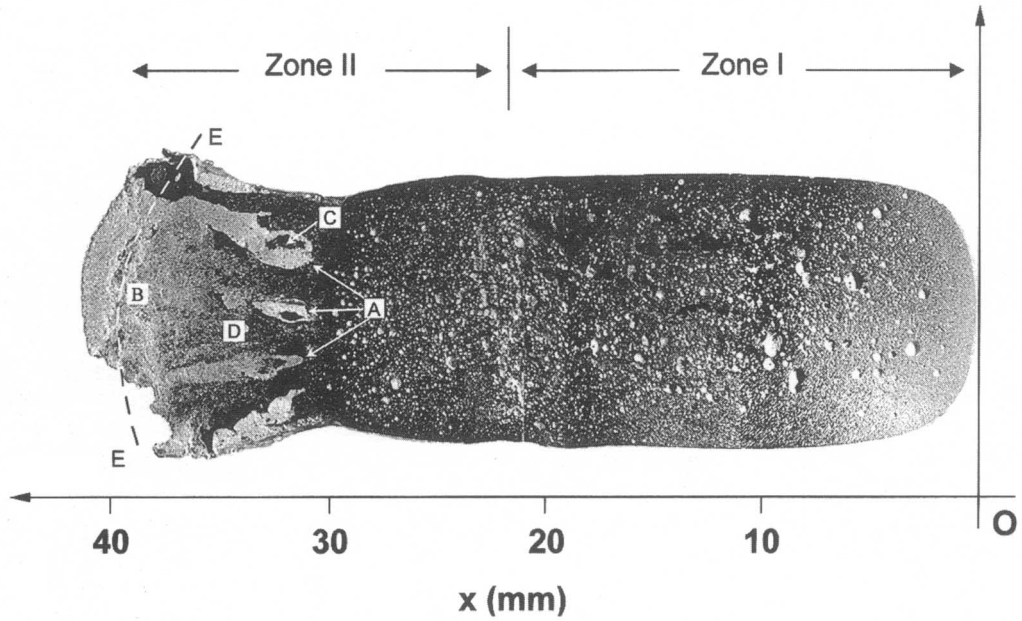

Fig. 2. Optical micrograph along the central longitudinal section of the semireacted bar shown in Fig. 1. Point O indicates the origin of a reference coordinate system; A, B, C, and D indicate microstructural features, which are described in the text.

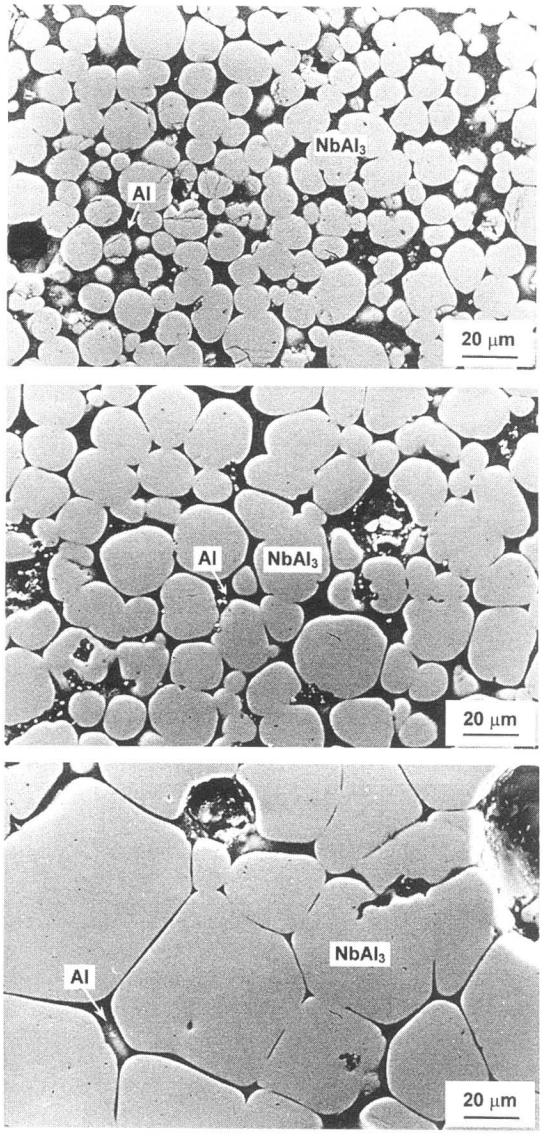

Fig. 3. SEM micrographs (backscattered electrons) of zone I from regions corresponding to (a) x = 0.5 mm, (b) x = 16 mm, and (c) x = 21 mm.

ones are voids of up to 1 mm. The small ones are about 2 μm. The average pore size is around 30 μm. Porosity is a consequence mainly of the fact that the reaction was performed under an argon atmosphere. Previous results of the present authors on compacted $NbAl_3$ pellets submitted to degassing before synthesis experiments, performed under vacuum, have shown that porosity can be drastically reduced [11].

Microstructural analysis executed along the longitudinal and transversal sections of the reacted bar revealed

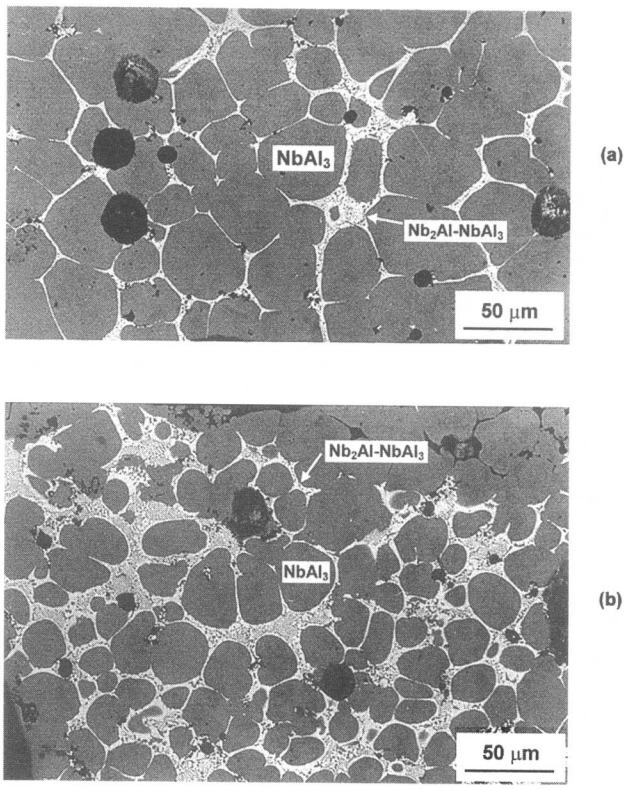

Fig. 4. SEM micrographs (backscattered electrons) of zone II from regions corresponding to (a) x = 24 mm and (b) x = 28 mm.

that the microstructure is very homogeneous along the (y, z) plane for any particular value of x between the origin and the necked region. In general, at this part of the reacted bar, a continuous variation of the microstructure is observed along the x direction. The microstructure of zone I ($0 \leq x \leq 22$ mm) is characterized mainly by the presence of particles (grains) of $NbAl_3$ surrounded by pure aluminum as can be seen from the micrographs in Fig. 3. As illustrated in this figure, when microstructural observations are made from the external surface (x = 0 mm) to the interior of the reacted pellet (increasing x), an increase in the volume fraction of $NbAl_3$ with a corresponding decrease in the volume fraction of aluminum is verified. Also, the morphology of the $NbAl_3$ particles changes from spheroidal to polyhedral, with a corresponding increase in size from 12 ± 3 to 47 ± 13 μm, as particle impingement increases. In the vicinity of zone II (x = 21 mm), $NbAl_3$ is the major phase and aluminum is present only at some few grain boundaries (Fig. 3c). Part of zone II, pertaining to the interval 22 mm $\leq x \leq$ 30 mm, is characterized by the presence of $NbAl_3$ particles and a

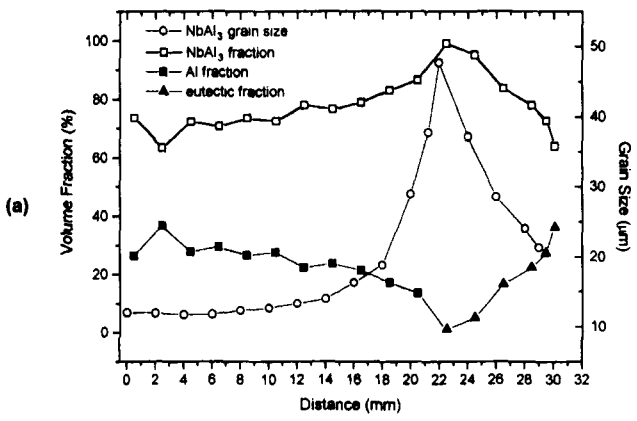

Fig. 5. (a) Volume fraction of $NbAl_3$, free aluminum, and eutectic, and average particle/grain size of $NbAl_3$; (b) weight fraction of aluminum and niobium along the longitudinal direction of the bar (position x) for zones I and II ($x \leq 30$ mm).

eutectic (Nb_2Al–$NbAl_3$) constituent as illustrated in the micrograph in Fig. 4a. In this region, when the observations are made at increasing values of x, the volume fraction of $NbAl_3$ decreases, with a concurrent increase in the volume fraction of the eutectic component. Also, the size of the $NbAl_3$ grains is decreased from 47 ± 13 μm at $x = 22$ mm to 21 ± 6 μm at $x = 30$ mm. These facts can be visualized in the micrographs presented in Figs. 4a and b for $x = 24$ mm and $x = 28$ mm. To illustrate these results better, the volume fraction of the various phases, the average particle/grain size of $NbAl_3$, and the weight fraction of aluminum and niobium are plotted as a function of position x in Figs. 5a and b, for zones I and II ($x \leq 30$ mm).

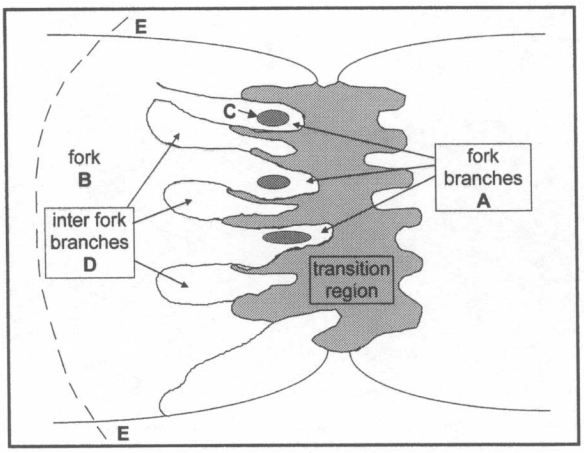

Fig. 6. Schematic representation of zone II showing the fork and interfork branch microstructure.

Beyond the necked region in zone II ($x \geq 30$ mm), the general microstructure is very complex and heterogeneous in the (y, z) plane. A schematic representation of this region is presented in Fig. 6. The most startling details in the microstructure of this region are a fork-like feature and a transition region. This fork-like feature, with fork branches pointing toward the necked region, is well evidenced by the white areas (noted A) in the macrograph in Fig. 2. Fork branches are seen to merge at B ($x \approx 40$ mm). Except for the dark areas inside the fork branches, labeled C in Fig. 2, the internal "fork branch" microstructure is characterized by the presence of very fine $NbAl_3$ grains, ≈ 5 μm in size, immersed in a continuous aluminum matrix, as can be seen in the micrograph in Fig. 7. Region C has a very complicated micro-

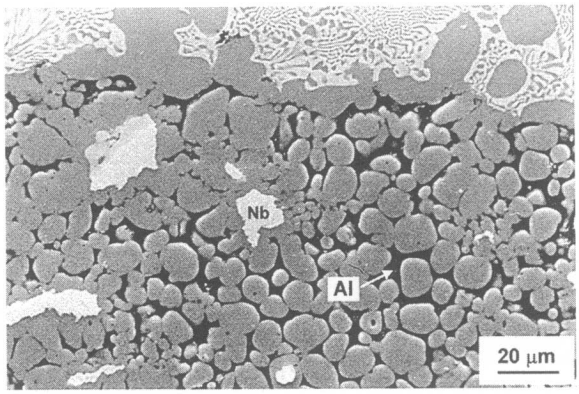

Fig. 7. SEM micrograph (backscattered electrons) from the inside of a fork branch, showing fine $NbAl_3$ grains in an aluminum matrix.

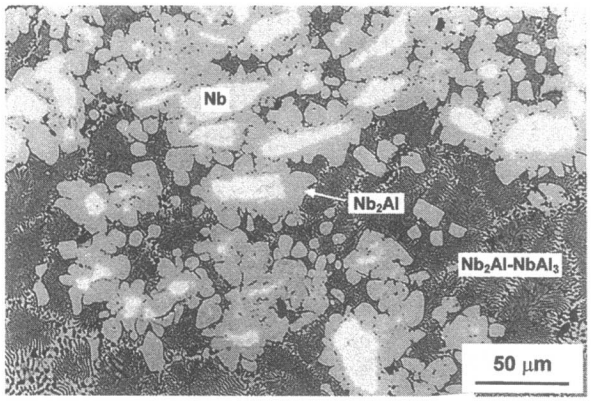

Fig. 8. SEM micrograph (backscattered electrons) from a dark region in Fig. 2 (label C).

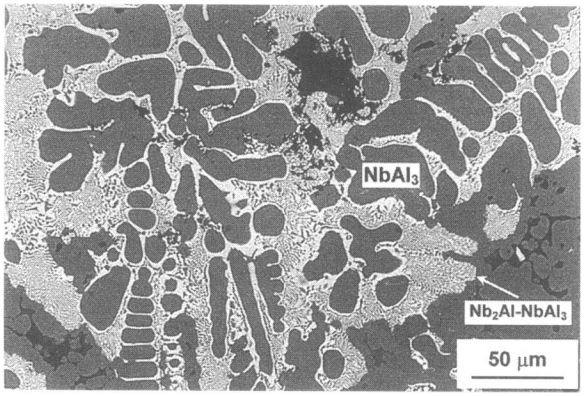

Fig. 10. $NbAl_3$ dendrites involved by the Nb_2Al–$NbAl_3$ eutectic (SEM backscattered micrograph).

structure consisting of nonreacted Nb and Nb_2Al particles embedded in the Nb_2Al–$NbAl_3$ eutectic as can be visualized as the light area in the SEM back-scattered micrograph in Fig. 8, which corresponds to the dark areas in the optical macrograph in Fig. 2. The inter-fork branch region (labeled D) shows the presence of larger $NbAl_3$ particles in a less continuous aluminum matrix. The SEM micrograph in Fig. 9 illustrates this inter-fork branch microstructure.

The well-delineated transition region around the necked area is characterized by the presence of $NbAl_3$ dendrites in a continuous Nb_2Al–$NbAl_3$ eutectic as shown in Fig. 10. This region contacts the fork branches to some extent and is bordered by the inter-fork branch area.

A very porous area (line E in Figs. 2 and 6) parallel to the wave propagation front is observed. The microstructure at the right side of the porous line consists of very fine $NbAl_3$ grains immersed in Al, similar to that shown in Fig. 3a. The area situated on the left side of the porosity line, near the reaction extinction front, is characterized by the presence of semireacted Nb particles surrounded by fine $NbAl_3$ grains, 4.3 μm in size, immersed in an aluminum matrix, as illustrated in the SEM back-scattered micrograph in Fig. 11.

Zone III is characterized by the presence of Nb and Al particles typical of the nonreacted compact, as can be verified in Fig. 12.

3.3. Progress of the Reaction (Step Sequence)

Possible steps involved in the reaction can be inferred from the results of phase identification along the bar, described above. The data in Fig. 5 suggest that

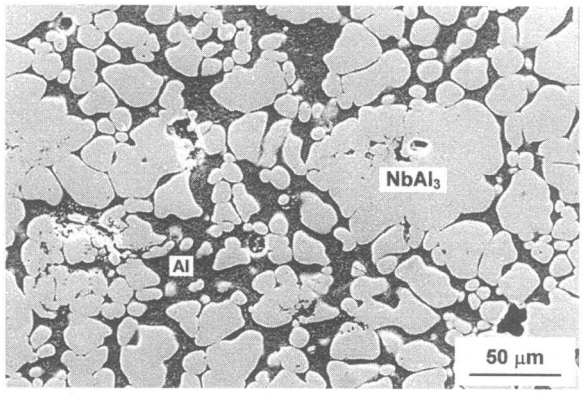

Fig. 9. SEM micrograph (backscattered electrons) of the inter-fork branch region. Large $NbAl_3$ grains in an aluminum matrix are shown.

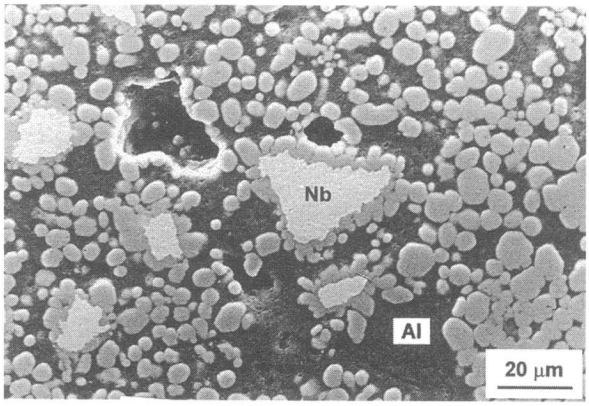

Fig. 11. Fine $NbAl_3$ grains present at the surface of semireacted niobium particles immersed in an aluminum matrix (SEM backscattered micrograph).

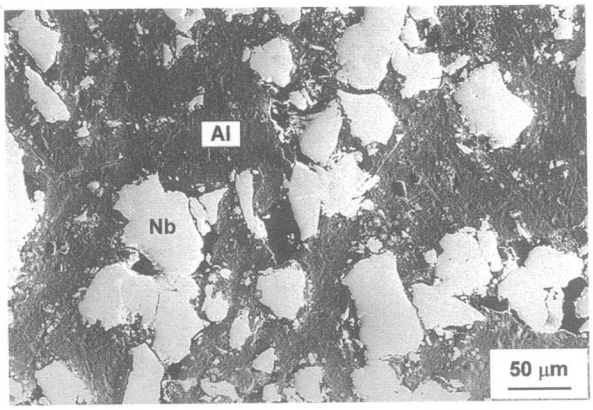

Fig. 12. *SEM micrograph (backscattered electrons) of a nonreacted region, showing Nb particles in an aluminum matrix.*

the region 0 mm $\leq x \leq$ 30 mm of the reacted bar can be visualized as being composed of several slices containing amounts of niobium and aluminum different from the initial (25Nb–75Al, at%) bar composition. Also, the bar composition is unbalanced during the reaction by an aluminum migration in the opposite x direction, that is, from zone II to zone I. The amount of aluminum carried out from one slice to another adjacent one depends on the particular slice position x.

This aluminum flux can probably be explained as resulting from the nonwetting characteristic of solid niobium by molten aluminum. In fact, that one-third of the bar introduced into the furnace in the beginning of the experiment evidenced the formation of aluminum droplets on its surface, as soon as the temperature in the region increased above the melting point of aluminum. Due to the temperature gradient along the bar, the internal region ahead of the first igniting slice will also contain some molten aluminum. Once ignition occurs in the first slice, the molten aluminum present in the droplets at the surface, as well as in the contiguous internal area, will be sucked to the reaction zone to feed the reaction. As a consequence of this aluminum transport, the real composition of most of zone I during the reaction will be richer in aluminum, above the initial 25Nb–75Al composition. As the combustion synthesis reaction propagates through zone II, outside the hot zone of the furnace, the heat generated by the reaction will give rise to a temperature increase in the region ahead of the reaction front, leading to aluminum melting in this area. In this way, the same mechanism will be operating and there will be a molten aluminum flux to the reaction zone as the reaction front advances.

In the region ahead of the reaction front, molten aluminum will be interacting with solid niobium. Inside these particular bar slices, the reaction can start. Reaction propagation to the next slice will depend on the amount of heat generated by the reaction. If this heat is not enough to increase the local temperature above the ignition temperature, the reaction will develop only partially or will be killed. The very heterogeneous region ahead of the bar necking is the result of the combined action of several factors: aluminum unbalancing, a temperature gradient, and lower heat generation. The fork and inter-fork branch regions could be the result of subsequent aluminum intrusions into the reaction zone due to the forward movement of the reaction front in the presence of a temperature gradient. In these two regions, corresponding to aluminum intrusions that occurred in two subsequent instants of time, the reaction started but was not taken to completion. Therefore, the area ahead of the bar necking corresponds to a frozen view of the last aluminum intrusions. The microstructures observed in these areas indicate that the reaction has, in fact, occurred at different times and taken to different levels. If it is assumed that the reaction front propagation velocity is practically constant, the time available for the reaction evolution should be the same for two contiguous slices. The region inside the fork branches, in which the maximum temperature attained is slightly over 660°C, will show the first reaction steps. The inter-fork region, being at a higher temperature, will show the reaction taken to a higher level or later stage due to the reaction kinetics. This would explain the presence of less nonreacted aluminum and larger $NbAl_3$ particles observed in this region (Fig. 9), compared to that inside the fork branch region (Fig. 7).

In a previous publication [11] by the present authors, it was suggested that the $NbAl_3$ synthesis reaction would occur by the initial niobium dissolution in molten aluminum followed by the precipitation of $NbAl_3$ on the surface of the nondissolved part of Nb particles. As can be noted in the micrograph in Fig. 11, taken in the region in which the reaction has just started and been interrupted, very fine $NbAl_3$ particles are present on the surface of dissolving niobium particles, indicating that this seems to be the case.

The occurrence of $NbAl_2$ and the eutectic inside small areas of the fork branches (Fig. 8) cannot be easily explained. A possible reason for this is the encounter of the advancing reaction front and the fork branches in the presence of a temperature gradient. As a result of the interaction of these two liquids, some poorer aluminum liquid pertaining to the transition region could be trapped inside the fork branches and its solidification,

under more critical conditions, would lead to the observations.

4. CONCLUSIONS

A simple device was built and utilized to perform interrupted SHS reactions on parallelopipedal $NbAl_3$ bars. Microstructural analysis conducted along a semireacted bar revealed the occurrence of a molten aluminum flux which causes a variation in the initial bar composition during the reaction propagation, leading to a microstructure gradient along the bar and also an extinction of the reaction propagation. The results suggest that the first reaction step probably occurs through a Nb dissolution in molten aluminum and reprecipitation of $NbAl_3$.

REFERENCES

1. V. Hlavacek, *Ceram. Bull.* **70**(2), 240 (1991).
2. Z. A. Munir, *Am. Ceram. Soc. Bull.* **67**(2), 342 (1988).
3. Z. A. Munir and U. Anselmi-Tamburini, *Mater. Sci. Rep.* **3,** 277 (1989).
4. H. C. Yi and J. J. Moore, *J. Mater. Sci.* **25**(2B), 1159 (1990).
5. J. W. Mccauley, *Ceram. Eng. Sci. Proc.* **11**(9–10), 1137 (1990).
6. R. W. Rice, *J. Mater. Sci.* **26,** 6533 (1991).
7. J. Subrahmanyam and M. Vijaykumar, *J. Mater. Sci.* **27,** 6249 (1992).
8. Z. A. Munir, *Rev. Particul. Mater.* **1,** 41 (1993).
9. R. M. Leal Neto and P. I. Ferreira, in *III Seminário sobre Metalurgia do Pó (IIIrd Seminar on Powder Metallurgy), Proceedings,* São Paulo, SP, Oct. 23–25, 1991 (Associação Brasileira de Metalurgia, São Paulo, SP, 1991), pp. 399–418.
10. R. M. Leal Neto and P. I. Ferreira, in *X Congresso Brasileiro de Engenharia e Ciência dos Materiais (Xth Brazilian Congress on Engineering and Materials Science), Proceedings, Vol. 2,* Águas de Lindóia, SP, Dec. 6–9 (1992), pp. 671–674.
11. P. I. Ferreira and R. M. Leal Neto, *Int. J. Powder Metall.* **30**(3), 313 (1994).
12. R. M. Leal Neto, J. G. B. Taveira, W. S. Inoue, and P. I. Ferreira, in *XI Congresso Brasileiro de Engenharia e Ciência dos Materiais (XIth Brazilian Congress on Engineering and Materials Science), Proceedings, Vol. 1,* Águas de São Pedro, SP, Dec. 11–14 (1994), pp. 107–110.
13. J. C. Murray and R. M. German, *Metall. Trans.* **23A**(9), 2357 (1992).
14. C. R. Kachelmyer, A. S. Rogachev, and A. Varma, *J. Mater. Res.* **10**(9), 2260 (1995).